Evaluation of Simulation Strategies for Multipoint Injection Systems in Aero-Engines on the Example of a Liquid Jet in a Gaseous Crossflow

F. Jaegle‡*, J.M. Senoner‡, M. García‡, C. Jiménez†, B. Cuenot‡, T. Poinsot‡
‡ CERFACS, 42 Av. Gaspard Coriolis, 31057 Toulouse, France
† Ciemat, Modeling and Numerical Simulation Group, Energy Dept., 28040 Madrid, Spain

Abstract

In an effort to reduce CO_2 and NO_X emissions of aeronautical engines, staged injection systems that allow optimizing lean combustion processes for different operating points are becoming more and more common. These systems employ multipoint injections where only the central part uses a classical hollow-cone fuel injection while for the second stage, a series of fuel jets are injected perpendicularly to the airflow. The present work evaluates the capability of different numerical strategies to simulate multipoint injectors. The evaluation is carried out using the test-case of a liquid jet in a gaseous crossflow for which experimental data are available [1]. The gas phase is simulated using the large eddy simulation (LES) solver AVBP, which has demonstrated its ability to predict unsteady reactive flows in complex geometries [2]. For the liquid phase, a Euler-Lagrange method is used. Models in the Lagrangian solver include a Stokes law with Reynolds correction for drag as well as a Spalding-type model for evaporation, with two-way coupling between the gaseous and the dispersed phase. Primary and secondary breakup are not taken into account, as their role in realistic applications (outside the near-injector region) is limited. Instead, polydispersion at the injection is based on the size distribution in the fully developed spray available from measurement data. The impact of this lack of detail is analyzed by comparison to the experiment. Further analysis focuses on the spatial distribution of droplets downstream of the injection, as well as diameter distribution. It is shown that the degree of physical detail is sufficient to obtain a proper representation of the spray generated by a multipoint-type injector in the areas of interest for combustion.

Introduction

The configuration of a liquid jet in a gaseous crossflow is a well-suited testcase for numerical and experimental studies of multipoint injection in aeronautical combustors. In this context, the liquid jet corresponds to a single injection hole of such an injector, which allows to analyze all important mechanisms in detail and with reduced complexity. The present work is aimed at the investigation of methods for numerical simulation of this application. An extensive experimental study under conditions typical for aeronautical engines has been published by Becker et al. [1] and will be used for comparison.

In literature [3, 4, 1, 5, 6], two main phenomena are identified to characterize the behavior of the liquid jet after injection. The first is column breakup, which occurs when surface waves on the liquid column are amplified and lead to its disintegration into ligaments and the subsequent formation of a spray. The second is called surface breakup and means the stripping of small droplets through shear from the liquid column. Wu et al [3] proposed a classification of the conditions under which one of the two mechanisms is predominant, depending on the aerodynamic Weber number based on the diameter of the liquid column and the gaseous velocity of the crossflow, $We_{ae} = \rho_g d_{inj} u_g^2/\sigma$, and the momentum flux ratio $q = \rho_l u_l^2/(\rho_g u_g^2)$. In the present study, the Weber Number is kept constant at values characteristic of realistic gas-turbine combustors, while the momentum flux ratio is varied to obtain cases which correspond to different breakup regimes.

Numerical studies of this problem may rely on several approaches. As primary and secondary breakup mechanisms play an important role, a direct simulation using an interface tracking method would capture most of the physics involved. However, such methods are out of reach for realistic applications because of the high computational cost. Two examples for simplifying approaches are Apte et al. [7] who use a Lagrangian method, neglect the liquid column but take secondary breakup into account, as well as Rachner et al. [8] who use a Lagrangian method combined with simple laws for drag and surface/column breakup derived from empirical correlations. In the targeted application of gas turbine combustors, breakup does not play an important role outside the near-field injection region

*Corresponding author, felix.jaegle@cerfacs.fr

which is why it is chosen to be neglected entirely for reasons of computational cost. The focus is on investigating injection methods in view of applying them to full multipoint injectors, considering far-field effects only.

The AVBP gaseous solver

The LES code AVBP explicitly solves the compressible Navier-Stokes equations with a centered finite-element scheme, which achieves third-order accuracy in both time and space [9, 2, 10]. Suffering from numerical oscillations, the scheme is stabilized using second-order and fourth-order artificial viscosities [11]. A standard Smagorinsky formulation is used to model subgrid-scale turbulence. Inlet and outlet boundary conditions are imposed using the NSCBC method [12, 13]. At the inlet, an anisotropic turbulence field is injected using the methods of [14] and [15]. Wall boundaries are modeled using logarithmic wall laws [16, 17].

Numerical methods for the dispersed liquid phase

The Eulerian solver for the gas phase can be coupled with two different approaches for the liquid phase. The first one is a Lagrangian particle tracking technique (Euler-Lagrange, EL), the second one a Eulerian representation of droplet sprays (Euler-Euler, EE). The latter is not considered in the present paper, a comparative analysis of both methods is part of ongoing work. It is assumed that (i) droplets are of spherical shape (ii) the droplet density is much larger than that of the carrier fluid, (iii) the droplets are dispersed and collisions can therefore be neglected, (iv) the droplets are much smaller than the LES filter width, (v) motion due to shear is negligible. The governing equations of motion for the liquid phase in the Lagrangian solver is presented in the following section. As evaporation is of very little influence in the present case, only the equations related to drag are shown. Details on evaporation can be found in [18]. A single droplet's evolution is governed by the following equations: $x_{p,i}$ are the components of the droplet position and $u_{p,i}$ its velocity components. The index "p" denotes droplet (or particle) properties, "g" the ones of the gaseous phase and "$g@p,i$" gaseous properties interpolated from nodal values to the position of a given particle, in this case using a Taylor interpolation method. The particle relaxation timescale τ_p is defined in equation (2).

$$\frac{dx_{p,i}}{dt} = u_{p,i} \qquad \frac{du_{p,i}}{dt} = \frac{1}{\tau_p}\left(\tilde{u}_{g@p,i} - u_{p,i}\right) + g_i \tag{1}$$

$$\tau_p = \frac{4}{3}\frac{\rho_p}{\rho_g}\frac{d_p}{C_D(\mathrm{Re}_p)\,|\tilde{u}_{g@p,i} - u_{p,i}|} \tag{2}$$

where C_D is the drag coefficient which depends on Re_p, the particle Reynolds number based on the droplet diameter d_p and the relative velocity of the surrounding gas [19]. ρ_p/ρ_g is the ratio of the liquid to the gaseous density and g_i the vector of gravitational acceleration.

The testcase

The computational domain is based on the experiments performed by Becker et al. [1]. It consists of a duct with rectangular cross-section of which the upstream and downstream in- and outflow parts have been truncated. Through a circular injection nozzle ($d_{inj} = 0.45\ mm$), placed on the centerline of the bottom surface, a plain jet enters the duct perpendicularly to the bulk velocity and is subsequently deflected and atomized. **Figure 1** gives an overview of the shape, the coordinate system and the exact dimensions of the computational domain.

In all cases considered here, the gaseous flow parameters are identical. The air flow is characterized by a bulk velocity of *100 m/s*, a pressure of *6 bar* and an air temperature of *290 K*. Due to the relatively long stretch of upstream duct in the test bench, it can be assumed that the flow inside the computational domain is fully turbulent. Therefore, turbulence injection is used as an inlet condition. The necessary input is obtained through a separate simulation of a periodic stretch of duct. This provides profiles of all mean and fluctuating velocity components as well as correlations for a LES flow field of the same filter width. The global Reynolds number of the flow, based on the channel width is $Re_g = 1 \cdot 10^6$. The mesh is of unstructured type, comprising approximately *320 000* nodes and *1.2* million grid cells. The mesh is refined towards the boundary layer with the first point situated at roughly *500* wall units.

The liquid injection is characterized by the momentum flux ratio $q = \rho_l u_l^2/(\rho_g u_g^2)$ between liquid and gaseous flow. Three different values of q (*2, 6* and *18*) are compared, resulting in different penetration heights, different breakup mechanisms and therefore different spatial and droplet diameter distributions in the spray.

Injection methods

This section describes the procedure to inject the liquid phase into the domain. In the simulation, primary and secondary breakup are not taken into account. Therefore, information on the polydiserse properties of the spray has to be determined in a different way: the experimental particle size distribution, measured on a plane at $x = 80$ *mm* downstream of the injection point at the height of the maximum volume flux, is taken as a reference on which droplet generation in the simulation is based. This corresponds to the fully developed spray that is assumed not to evolve further after injection. It has to be noted that the experimental diameter distribution obtained on a single point is not necessarily representative of the global distribution. On the other hand, Becker et al. [1] compared the spatial evolution of several representative diameters in the spray and suggest that the local size distribution can be assumed to be similar throughout the spray. It will be shown that an injection procedure based on these simplifications still yields satisfactory results and can be justified for the use in industrial applications.

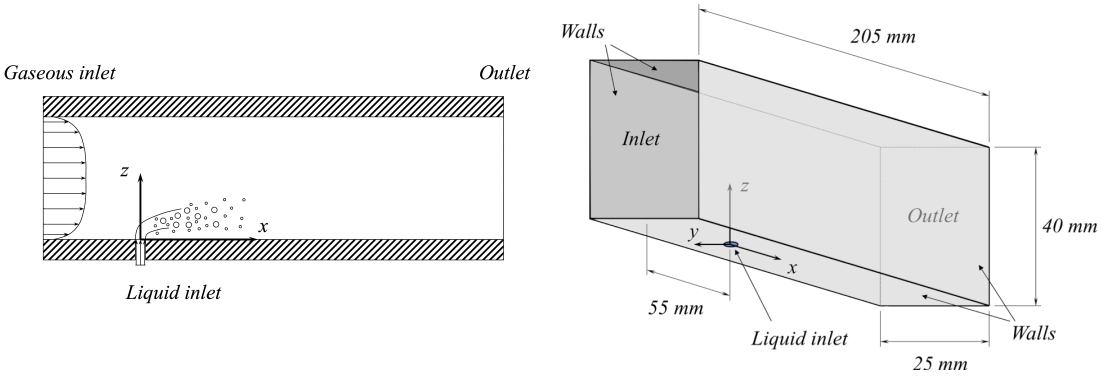

Figure 1. Schematics of the computational domain. Left: cross-section on the mid-plane (y=0). Right: isometric view (from below) with dimensions.

A first, very simple method to be tested consists in injecting droplets on a circular patch corresponding to the inlet section of the liquid jet. Individual droplets are randomly placed on this patch and assigned a random diameter weighted by a log-normal distribution that has been fitted to the experimental data (**Figure 2**). Becker et al. [1] state that characteristic diameters of the spray depend mainly on the dynamic pressure of the airflow but show only very weak dependence on the liquid injection velocity. Therefore, the reference droplet size distribution [1] (measured for $q = 6$ at $x = 80$ *mm*) is also used for the cases of $q = 2$ and $q = 18$. The injection velocity is superimposed with 20% fluctuations normal to the jet axis to force the opening of the spray. This is deemed necessary for two reasons: first, with the current numerical approach, turbulent dispersion is under-estimated because droplets encounter a filtered LES velocity field. Second, breakup processes, which are neglected here, would lead to a further separation of droplet trajectories and thus to a more pronounced opening of the jet.

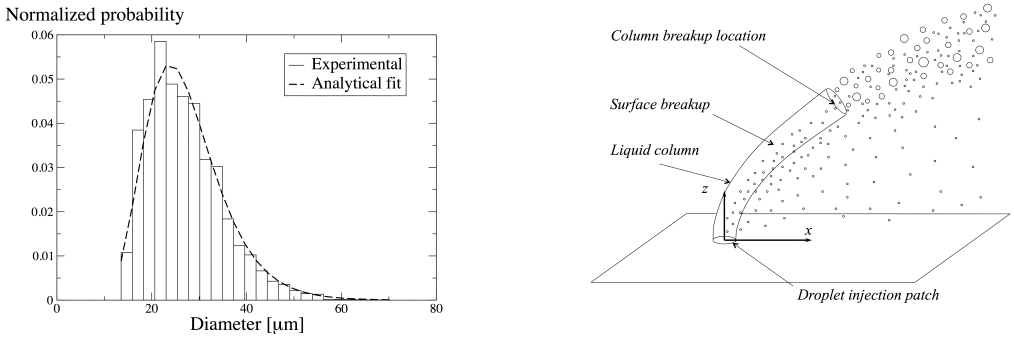

Figure 2. Left: diameter distribution on injection, analytical fit of a log-normal distribution to the experimental data [1] ($q = 6$) as used as input for all cases; Right: illustration of the liquid column model.

Injecting droplets directly at the jet nozzle without further physical consideration, i.e. neglecting the presence of a liquid column, will lead to droplet trajectories that are strongly deflected for small diameters and to such that penetrate relatively far in the case of large droplets. These trajectories will not necessarily correspond to a realistic behavior as small droplets can also result from secondary breakup at a certain distance from the injection. Furthermore, the drag coefficients of a liquid column and a droplet differ which leads to unphysical trajectories in the liquid column region.

A method inspired by the work of Rachner [8] is aimed at mitigating the said difficulties. This injection procedure estimates the length of the liquid column based on empirical correlations for the breakup location, as provided by Fuller et al. [6]. An overview of the different zones can be found in the right half of **Figure 2**. All droplets that are generated on the injection patch are initially assigned a drag coefficient of a liquid column element at the diameter of the injection nozzle. This drag coefficient can be obtained using the correlations presented by Fuller et al. [6]. These authors assume a mean drag coefficient over the length of the column and that forces are parallel to the freestream, which implies that drag in wall-normal direction is negligible. This modified law for particle drag is applied on all particles (regardless of their actual diameter), which have not yet gone beyond the estimated point of column breakup. Once droplets clear the liquid column area, they regain their intended properties, in particular their original drag based on particle diameter. Inside the liquid column region, all droplets will follow approximately the same trajectory, which corresponds to that of the liquid column. Two-way coupling terms in this area are masked.

A secondary treatment, which is a part of the model, reconstructs effects of surface breakup. The liquid mass removed from the column per unit length can be determined by an analytical analysis of liquid boundary layer stripping developed by Ranger and Nicholls [20]. A relation for the characteristic diameter of the droplets generated through shear can be obtained from the paper of Chou et al. [21]. In practice, a proportion (determined by the liquid mass stripped over the entire column length) of those droplets generated on the injection patch that have the characteristic diameter of surface breakup is flagged and subsequently released from the column at a random location along the column trajectory between injection and the location of column breakup.

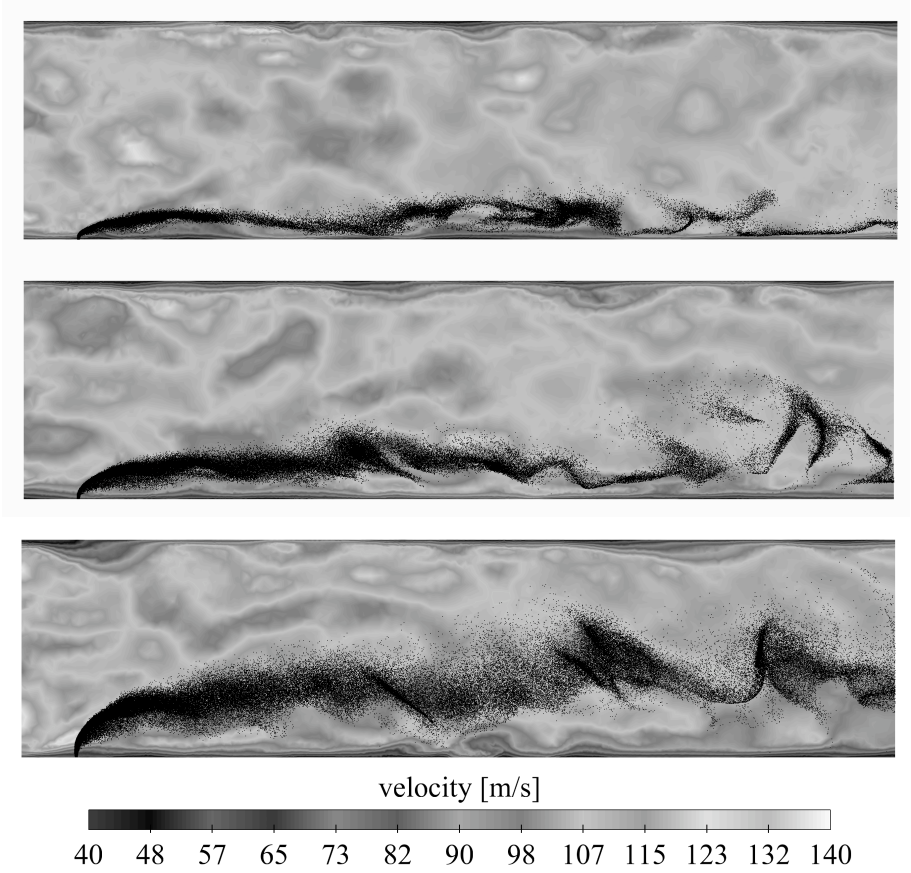

Figure 3. Instantaneous views of the cases $q = 2$, $q = 6$ and $q = 18$ (top to bottom). Cross section ($y = 0$) through the field of the axial velocity u_1, overlaid with particles in proximity of *1 mm* from the plane $y = 0$.

Results and Discussion

As a first, qualitative analysis of the liquid phase behavior, instantaneous views of all three cases, *q = 2, 6* and *18*, are considered. The results, shown in **Figure 3** have been obtained with the liquid column model. For all cases, a field of axial velocity on the mid-plane *y = 0,* overlaid with dots representing the particles inside a slice of 1 mm thickness in front of the mid-plane. A strong influence of the turbulence on the particles can be observed in all cases. In the case of *q = 18*, the liquid column region can be distinguished as a zone of a very compact bundle of droplet trajectories, trailed by a relatively sparse wake of droplets from surface breakup. For *q = 2* and *q = 6*, the liquid column is very short and therefore barely visible.

Quantitative analysis focuses on two aspects. The first is a comparison of the liquid volume flux $\Phi_{LV} = \alpha_l u_l$ to experimental data [1]. **Figure 4** shows the distribution of volume flux over the *z*-coordinate, measured at *x = 80 mm*, which allows to compare the jet penetration distance as well as the dispersion of the spray plume with the experiment. It can be noted that, for the results obtained without the liquid column model, the positions of the maxima are well reproduced for *q = 2*, slightly less so for *q = 6* whereas for *q = 18*, a clear underestimation can be observed. This is because, for high injection velocities, the reduced initial drag in z-direction that distinguishes the liquid column from spherical droplets, has an increased influence on penetration height. The application of the column model provides the expected increase of penetration height and even exposes a tendency to slight over-estimation.

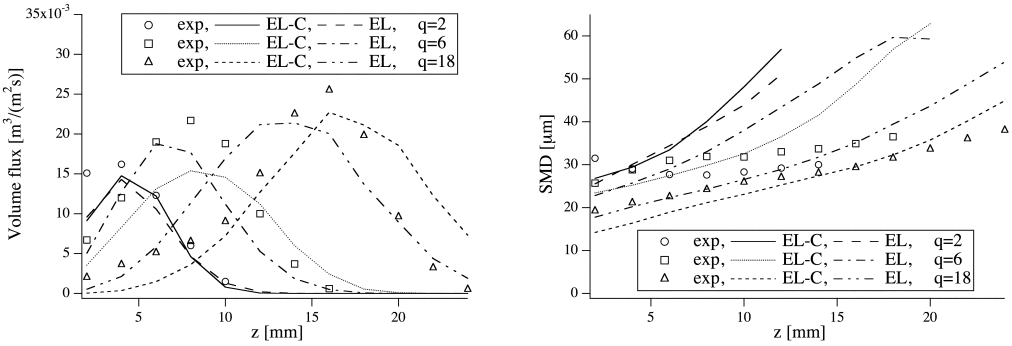

Figure 4. Comparison of LES results to experimental data [1]. "–C" marks cases using the liquid column model. Left: liquid volume flux at *x*=80 mm. Values extracted from the mean solution at different *z*-coordinates and averaged over *y*. Right: SMD at different *z*-coordinates from the mean solution. Values weighted with local liquid volume flux and averaged over *y*.

The second aspect to be compared to experimental data is the evolution of the Sauter mean diameter (SMD) over the z-coordinate at *x = 80 mm*, shown in the right part of **Figure 4**. In the cases without column model, there is generally good agreement at the *z*-location of maximum fuel flux with a clear over-estimation of SMD above this position. This is due to small droplets failing to reach these heights as they begin to be decelerated starting from *z=0*. In reality, there is, however, a certain amount of small droplets that is generated after the disintegration of the liquid column (which occurs well above the injection height), through the fragmentation of ligaments and secondary breakup of larger drops. The liquid column model captures this effect in part, as it lets droplets of all diameters follow common trajectories and releases them at the location of secondary breakup. Consequently, the agreement with experimental data is improved in the neighborhood of maximum fuel flux. The influence is strongest for *q = 18* while for *q = 2*, no pronounced effect can be observed.

Below the *z*-coordinate of maximum fuel flux, the experimental profiles show an increase of SMD towards the wall. Becker et al. [1] explain this effect as an influence of the boundary layer: for low values of *q*, large droplets from the disintegrated column may be positioned low enough to be exposed to the reduced gas phase velocity in the boundary layer. As a result, secondary breakup is not as effective as in the free flow leading to the observed increase of SMD. In the simulations, this effect is not captured at all due to the absence of secondary breakup mechanisms.

The inclusion of surface breakup into the liquid column model does not yield conclusive effect on the results. For *q = 2* and *q = 6*, the slope of SMD evolution is reduced in the lower *z*-coordinates where surface breakup is active. This indicates that the spray in this region contains a larger proportion of droplets from surface breakup with its narrow diameter band, as opposed to the purely ballistic separation of diameter classes that governs the spray composition in the absence of the column model. However, as the increase of SMD due to the boundary layer appears to

be the dominant effect in experimental data for lower values of q, it is difficult to assess potential improvements from the surface breakup component in the simulations. For $q = 18$, the SMD in the lower z-regions decreases as a result of surface breakup, but the overall shape of SMD evolution remains in good agreement with experimental data.

Conclusion

Simulations of a liquid jet's injection into a gaseous crossflow have been carried out using a Euler-Lagrange formulation, coupled with the AVBP gaseous solver. Two simple methods for injection were compared, the first of which does not account for primary and secondary breakup processes. The second uses a simple procedure for the liquid column that is based on empirical correlations. In both cases, information on polydispersion was reconstructed from measurement data. Comparison to experimental data by Becker and Hassa [1] regarding the spatial distribution of liquid volume flux and the evolution of the Sauter mean diameter (SMD) has been made for different values of the momentum flux ratio q. The main findings are: there is generally good agreement with experimental data but the high degree of simplification of the most basic injection method reveals shortcomings regarding penetration height (at high values of q) and SMD distribution for low values of q. To a certain degree, these deficiencies could be improved by the application of a liquid column model.

Acknowledgements

F.J. and J.M.S. gratefully acknowledge the support of the European Community in the framework of the Marie Curie Early Research Training Fellowship (contract number MEST-CT-2005-020426).

References

1. Becker, J., and Hassa, C., *Atomization and Sprays,* 11:49–67, (2002).
2. Moureau, V., Lartigue, G., Sommerer, Y., Angelberger, C., Colin, O., and Poinsot, T., *Journal of Computational Physics*, 202(2):710–736, (2005).
3. Wu, P. K., Kirkendall, K. A., and Fuller, R. P., *Journal of Propulsion and Power.* 13:64–73, (1997).
4. Chen, T. H., Smith, C. R., and Schommer, D. G., *AIAA Paper,* 93-0453, (1993).
5. Adelberg, M., *AIAA Journal.* 6:1143–1147, (1968).
6. Fuller, R. P., Wu, P. K. and Kirkendall, K. A., *AIAA Journal.* 38:64–72, (2000).
7. Apte, S. V., Gorokhovski, M., and Moin, P., *Int. Journal of Multiphase Flow.* 29:1503–1522, (2003).
8. Rachner, M., Becker, J., Hassa, C., and Doerr, T., *Aerospace Science and Technology,* 6:495–506, (2002).
9. Schönfeld, T., and Rudgyard, M., *AIAA Journal*, 37(11):1378–1385, (1999).
10. Colin, O., and Rudgyard, M., *Journal of Computational Physics*, 162(2):338–371, (2000).
11. Lamarque, N. "Schémas numériques et conditions limites pour la simulation aux grandes échelles de la combustion diphasique dans les foyers d' hélicoptère" Institut National Polytechnique de Toulouse, PhD thesis No. TH/CFD/07/117.
12. Poinsot, T., Lele, S., *Journal of Computational Physics* 101(1):104–129, (1992).
13. Poinsot, T. and Veynante, D., *Theoretical and numerical combustion*. R.T. Edwards, 2nd edition, 2005.
14. Kempf, A., Klein, M. and Janicka, J., *Flow, Turbulence and Combustion*, 74:67–84, (2005).
15. Kraichnan, H., *Physics of Fluids,* 13(1):22–31, (1970).
16. Schmitt, P. "Simulation aux grandes échelles de la combustion étagée dans les turbines à gaz et son interaction stabilité - polluants - thermique" Institut National Polytechnique de Toulouse, PhD thesis No. TH/CFD/05/45.
17. Schmitt, P., Poinsot, T., Schuermans, T. J., and Geigle, K., *Journal of Fluid Mechanics,* 570:17–46, (2007).
18. Boileau, M., Pascaud, S., Riber, E., Cuenot, B., Gicquel, L.Y.M., Poinsot and T. Cazalens, M., *Flow, Turbulence and Combustion*, 80(3):291–321, (2008).
19. Schiller, L., and Nauman, A., *VDI Zeitung*, 77:318–320, (1935).
20. Ranger, A. A. and Nicholls, J.A., *AIAA Journal*. 7(2):285–290,(1969)
21. Chou, W. -H., Hsiang, L. -P. and Faeth, G. M., *Int. journal of Mulitiphase Flow*. 23(4):651–669, (1997)